

Electronic Supplementary Information

Anti-fluorite Li_6CoO_4 as an alternative lithium source for lithium ion capacitors: An experimental and first principles study

Young-Geun Lim,^{a,e,‡} Duho Kim,^{b,‡} Jin-Myoung Lim,^b Jeom-Soo Kim,^{a,d} Ji-Sang Yu,^a
Young-Jun Kim,^a Dongjin Byun,^e Maenghyo Cho,^b Kyeongjae Cho^{*,b,c} and Min-Sik Park^{*,a}

Eqn. S1 Calculation of theoretical capacity of Li_6CoO_4

$$\begin{aligned} Q &= nN_A e = nF = n \times 96485.34 \text{ C} \cdot \text{mol}^{-1} \quad (n = 6 \text{ mol of electrons in } \text{Li}_6\text{CoO}_4) \\ &= 578912.04 (\text{A} \cdot \text{s}) \cdot \text{mol}^{-1} \\ &= 578912.04 \left(1000 \text{ mA} \cdot \frac{1}{3600} \text{ h} \right) \cdot \text{mol}^{-1} \\ &= 578912.04 \text{ mAh} \cdot \text{mol}^{-1} \\ &= \frac{160808.9}{164.5768} \text{ mAh} \cdot \text{g}^{-1} \\ &= 977 \text{ mAh} \cdot \text{g}^{-1} \end{aligned}$$

where, N_A is the Avogadro's number, e the electric charge of an electron, F the Faraday constant, A the ampere, s the second, and 164.5768 the molecular weight of Li_6CoO_4 .

Eqn. S2 Average Coulomb interaction energy

The average coulomb interaction energy for N ions in tetrahedral geometries of Li-O (nearest neighbor interactions), at positions $r_1; r_2; \dots; r_N$, and occupying point charges $q_1; q_2; \dots; q_N$, can be described as below.

$$E_c = \frac{1}{4\pi\epsilon_0} \left(\frac{1}{(N-1)} \frac{q_i q_j}{|r_{ij}|} \right)$$

Where $r_{ij} = r_i - r_j$ is the bond length of Li-O, ϵ_0 is an electric constant ($8.854 \times 10^{-12} \text{ C}^2 \text{ N}^{-1} \text{ m}^{-2}$).

Eqn. S3 Relative formation energy

The relative formation energy can be expressed as:

$$E_f^r = E_{tot}[Li_{6-x_1}CoO_4] - \left(\left(\frac{x_2 - x_1}{x_2} \right) E_{tot}[Li_6CoO_4] + \left(\frac{x_1}{x_2} \right) E_{tot}[Li_{6-x_2}CoO_4] \right)$$

where x_2 is the number of finally extracted Li^+ , x_1 is the number of partially extracted Li^+ and E_{tot} refers to the total energy of $Li_{6-x}CoO_4$. To obtain more realistic thermodynamic quantities, Li^+ is sequentially extracted from the structure in all calculations.

Eqn. S4 Formation energy

The formation energy of partially de-lithiated states can be expressed as:

$$E_f = E_{tot}[Li_{x_1}CoO_4] - E_{tot}[Li_{x_2}CoO_4] + (x_1 - x_2)E[Li]$$

where x_2 is the number of Li^+ in the fully lithiated state and x_1 is the number of Li^+ located in the intermediate de-lithiation state. $E[Li]$ is the chemical potential of metallic lithium in the bcc structure.

Table S1. Summary of physical and electrochemical characteristics for activated carbon and hard carbon.

	PE (MSP-20)	NE (Hard carbon)
Avg. Particle size (μm)	9.0	9.8
Tab density ($\text{g}\cdot\text{cc}^{-1}$)	0.35	0.86
BET ($\text{m}^2\cdot\text{g}^{-1}$)	2156	2.28
Charge capacity ($\text{mAh}\cdot\text{g}^{-1}$)	86.4	315.7
Discharge capacity ($\text{mAh}\cdot\text{g}^{-1}$)	85.2	231.5
Coulombic Eff. (%)	98.6	73.3
Voltage Window (ΔV)	3.9 – 1.5	1.5 – 0.01
40C Retention (% vs. 0.2C)	61.1	27.8

Table S2 Specifications of the positive electrode (PE) and negative electrode (NE) for LICs.

Specification	PE (Conventional)		PE (Li_6CoO_4) 60% Doping		PE (Li_6CoO_4) 100% Doping		NE		
	weight (mg)	wt%	weight (mg)	wt%	weight (mg)	wt%	weight (mg)	wt%	
Active Material	5.805	92	5.805	80.9	5.805	74.8	3.36	80	
Composition	LCO	0	0	0.8	11.1	1.335	17.2	-	-
	Super-P	0	0	0	0	0	0	0.42	10
	PVdF	0.505	8	0.574	8.0	0.621	8.0	0.42	10
	Total	6.31	100	7.18	100	7.761	100	4.20	100
Loading level (mg cm^{-2})	5.58		6.35		6.86		2.73		
Electrode density (g cm^{-3})	0.5		0.5		0.5		0.8		

Table S3 Results of inductively coupled plasma (ICP) analysis for Li₆CoO₄.

Elements	Content (ppm)	Weight (g)	wt%	mol%	Li Fraction (vs. Co)
Li	259804	21.27	25.98	306.46	6.09
Co	362445	29.67	36.24	50.35	

Table S4 Results of ex-situ ICP analysis for Li_{6-x}CoO₄ obtained at various SOC.

SOC (%)	Elements	ppm (mg·kg ⁻¹)	Weight (g)	wt %	mol %	Li-contents	Extraction Value (x)
0	Li	180416.6	14.77	18.04	212.81	6.10	0
	Co	250974.1	20.55	25.10	34.87		
25	Li	162890.2	13.34	16.29	192.14	5.11	0.89
	Co	270453.5	22.14	27.05	37.57		
50	Li	158116.3	12.95	15.81	186.51	4.16	1.84
	Co	322679.4	26.42	32.27	44.83		
75	Li	109063.5	8.93	10.91	128.65	3.14	2.86
	Co	295358.4	24.18	29.54	41.03		
100	Li	132516.9	10.85	13.25	156.31	2.23	3.77
	Co	503717.4	41.24	50.37	69.98		

Table S5 Ionic conductivity of LICs during the 4.3 V pre-doping and subsequent discharge.

	LIC w/o Li ₆ CoO ₄ (mS·cm ⁻¹)	LIC with Li ₆ CoO ₄ (mS·cm ⁻¹)
OCV	11.52	11.52
4.3 V Charge (Pre-doping)	11.49	11.50
1.5 V Discharge	11.51	11.51

* Cell constant (l/A) = 99.1 m⁻¹

The galvanostatic charge and discharge profiles of LIC measured in mAh can be automatically converted to Wh using a cell tester (MACCOR series 4000, USA). Energy (Wh) can be derived from integration of the obtained charge and discharge profiles of LIC. Power (W) is calculated from the rate capability data using the equation below.

$$W = Wh \times \left(\frac{3600 \text{ sec}}{T_R} \right)$$

where Wh is energy obtained at each C rate (current density), and T_R is the real reaction time measured at each C rate.

For gravimetric energy and power calculations, total weight of PE (activated carbon + Li_6CoO_4 + conductor + binder + current collector), NE (hard carbon + conductor + binder + current collector), and separator were considered. The weight of electrolyte and exterior materials did not reflected for relative comparison. The volumetric energy and power were also calculated in same manner.

Table S6 Detailed information of PE and NE (gravimetric).

Specification	LIC – Conventional		LIC – Li_6CoO_4 60% doping		LIC – Li_6CoO_4 100% doping	
	PE (mg)	NE (mg)	PE (mg)	NE (mg)	PE (mg)	NE (mg)
Active material	5.805	3.360	5.805	3.360	5.805	3.360
LCO	0	0	0.800	0	1.335	0
Super-P	0	0.420	0	0.420	0	0.420
PVdF	0.505	0.420	0.574	0.420	0.621	0.420
Current collector	5.893	27.42	5.893	27.42	5.893	27.42
Separator		4.354		4.354		4.354
Total (mg)		48.174		49.043		49.628

Table S7 Detailed information of PE and NE (volumetric).

Specification		LIC – Conventional	LIC – Li_6CoO_4 60% doping	LIC – Li_6CoO_4 100% doping
		PE	0.01116	0.01270
NE		0.003	0.003	0.003
Thickness (cm)	Metallic Li	0.026 (1ea)	0	0
	Separator	0.0028 (2 ea)	0.0014 (1 ea)	0.0014 (1 ea)
	Total	0.04286	0.0171	0.0181
	Area (cm ²)	5.76	2.25	2.25
Volume (cm ³)		0.2469	0.0385	0.0407

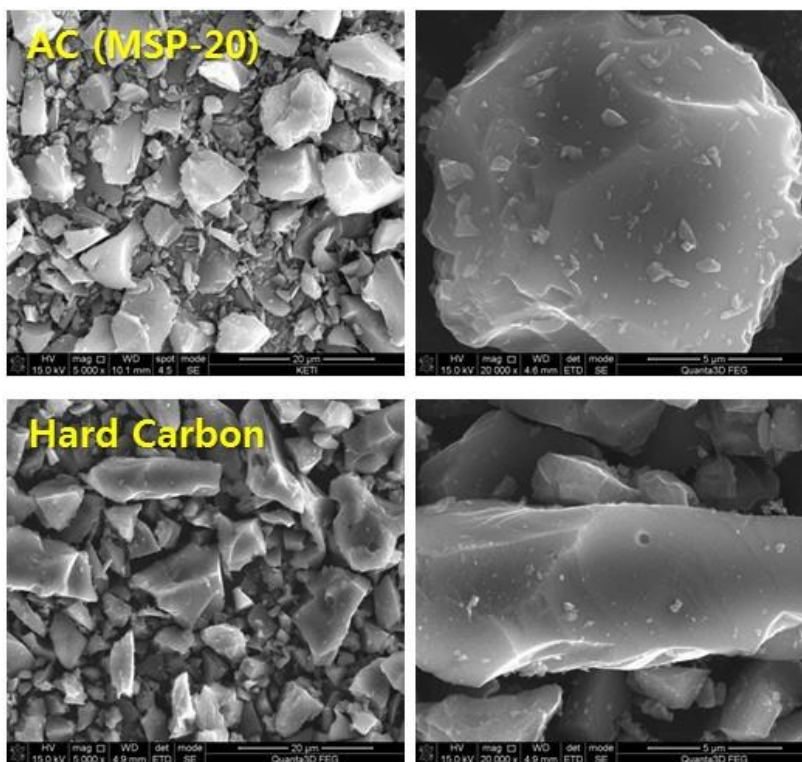


Fig. S1 FESEM images of activated carbon and hard carbon used in this work.

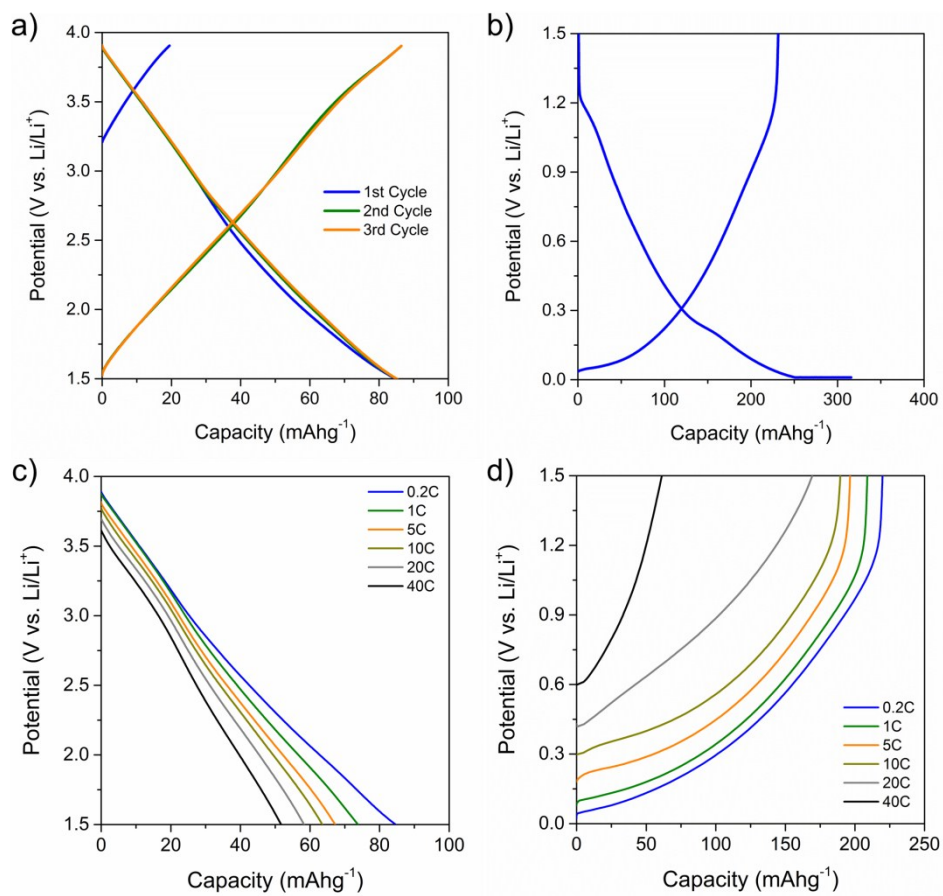
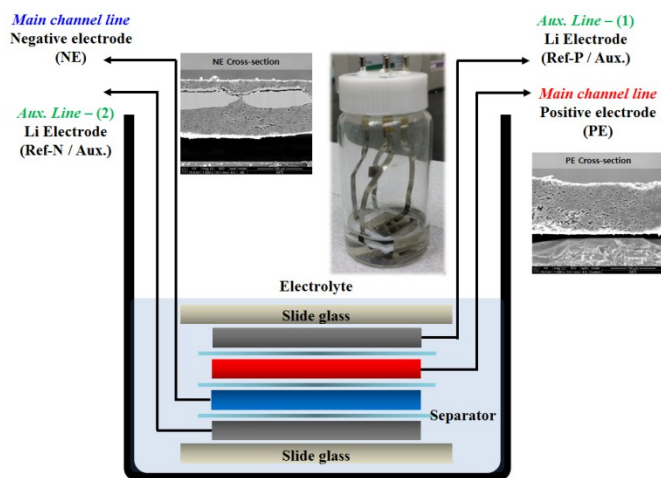
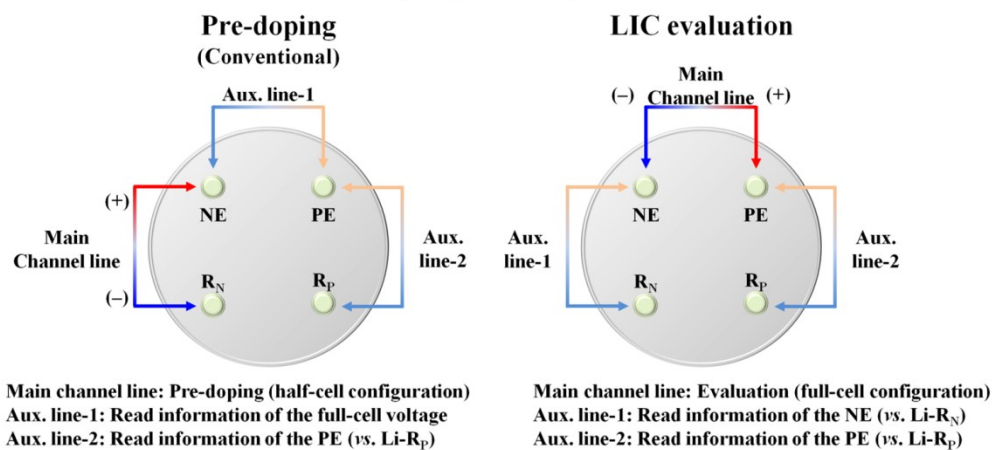


Fig. S2 Electrochemical characteristics of activated carbon and hard carbon used in this work; Galvanostatic charge and discharge profiles of (a) activated carbon PE and (b) hard carbon NE, and rate-capabilities of (c) activated carbon PE and (d) hard carbon NE at different current densities.

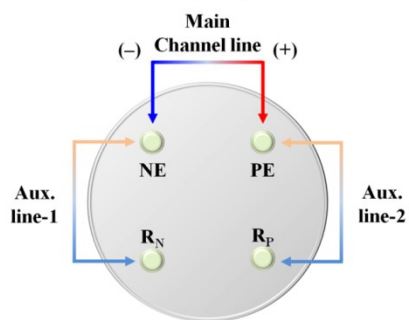
[Cross-sectional View]



[Top-View]



Pre-doping & LIC evaluation (Li₆CoO₄)



Main channel line: Evaluation (full-cell configuration)
Aux. line-1: Read information of the NE (vs. Li-R_N)
Aux. line-2: Read information of the PE (vs. Li-R_p)

Fig. S3 4-electrode cell configuration composed of PE, NE, and two Li electrode as reference electrodes.

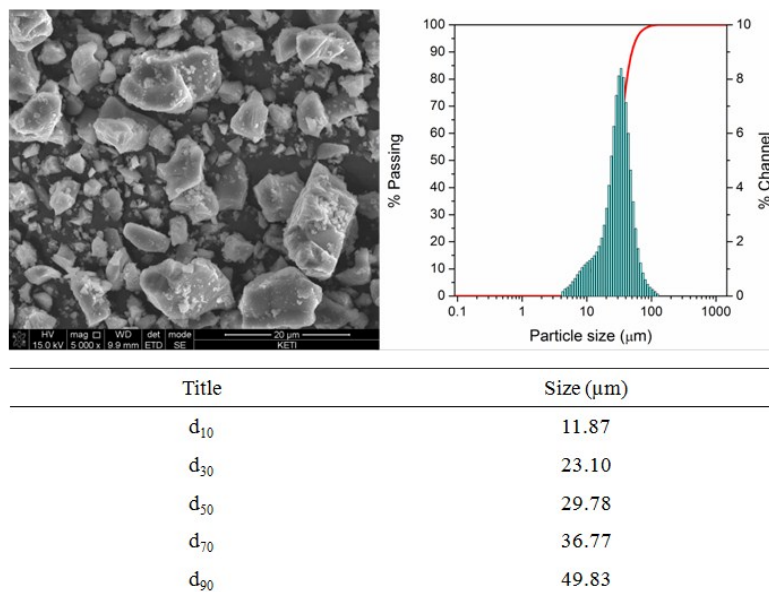


Fig. S4 A FESEM image and particle size distribution (PSA) of as-prepared Li_6CoO_4 particles together with selected measured values.

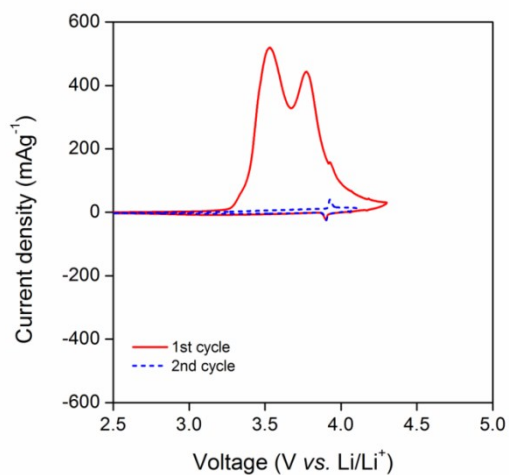


Fig. S5 Cyclic voltammograms of Li_6CoO_4 recorded with a scan rate of 0.05 V s^{-1} in a voltage range of 2.5 to 4.3 V vs. Li/Li^+ at the first and second cycles.

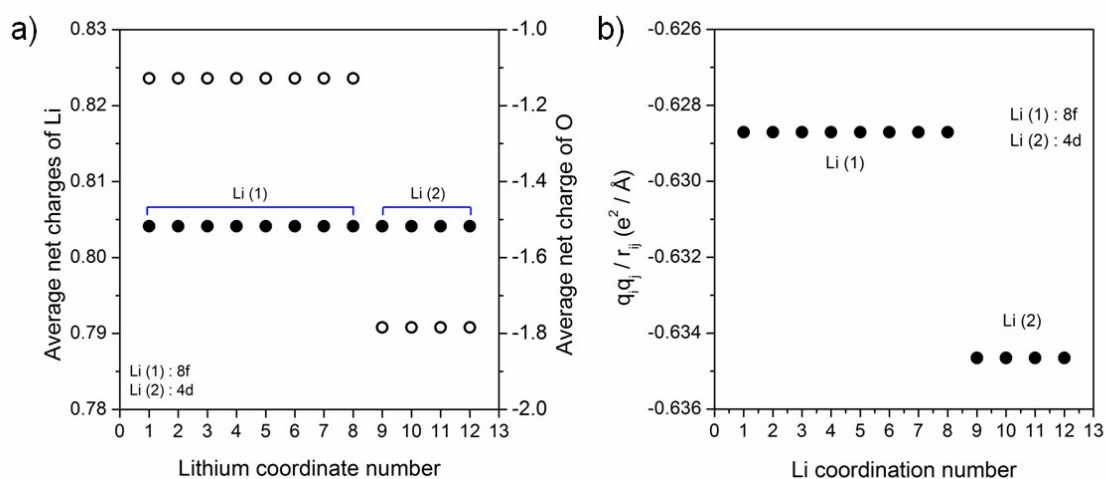


Fig. S6 (a) Average net charges of Li and O, and (b) attractive pair electrostatic interaction in all Li positions on the Li_6CoO_4 structure.

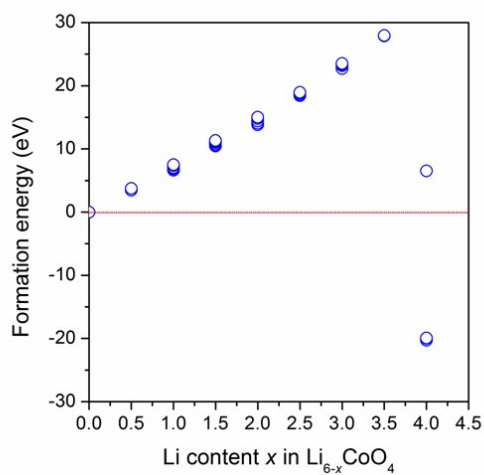


Fig. S7 Formation energy of $\text{Li}_{6-x}\text{CoO}_4$ with different Li contents from $x = 0$ to 4.0.

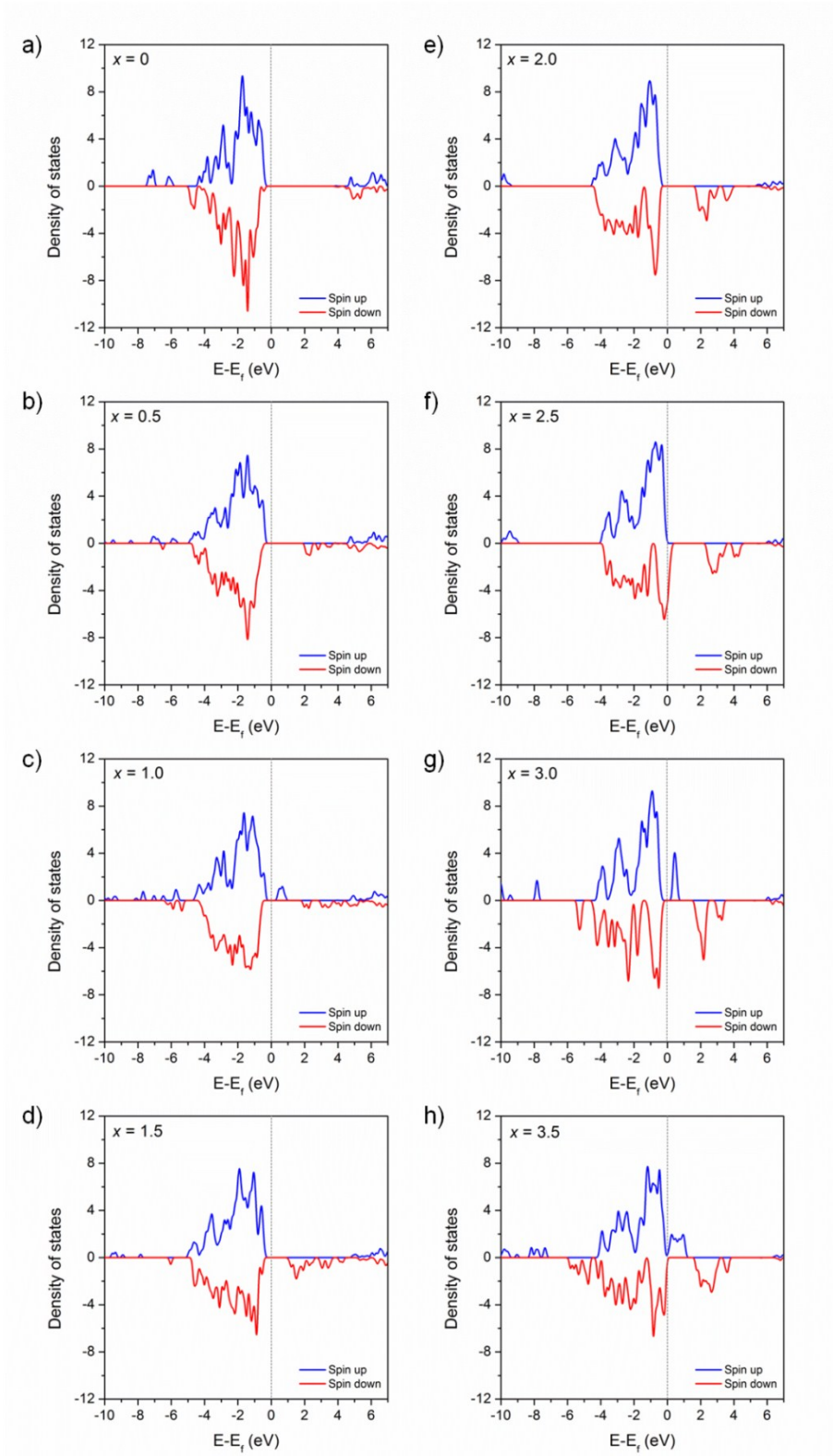


Fig. S8 O 2p partial density of state (PDOS) of $\text{Li}_{6-x}\text{CoO}_4$ with different Li contents; (a) $x = 0$, (b) $x = 0.5$, (c) $x = 1.0$, (d) $x = 1.5$, (e) $x = 2.0$, (f) $x = 2.5$, (g) $x = 3.0$, and (h) $x = 3.5$ (the dot-line indicates the Fermi level).

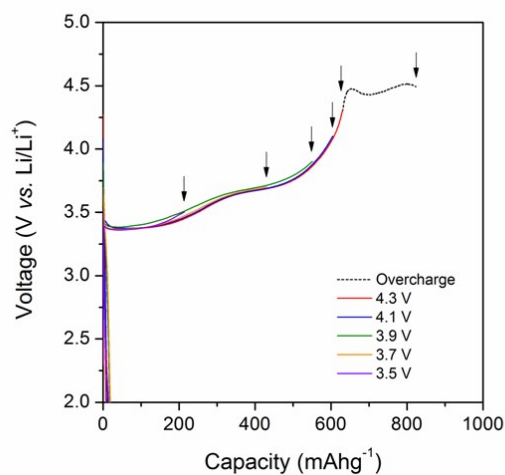


Fig. S9 Galvanostatic charge profiles of Li_6CoO_4 with different cut-off voltages: 3.5, 3.7, 3.9, 4.1, 4.3, and 4.5 (overcharged) V vs. Li/Li^+ .

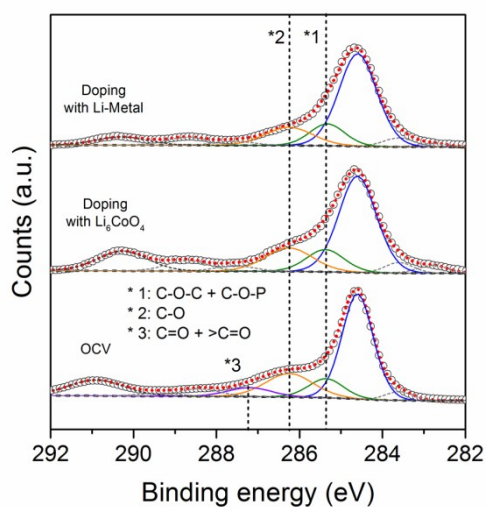


Fig. S10 *Ex-situ* XPS spectra of C 1s for the NEs after Li^+ pre-doping process with different pre-doping methods; metallic Li and Li_6CoO_4 .

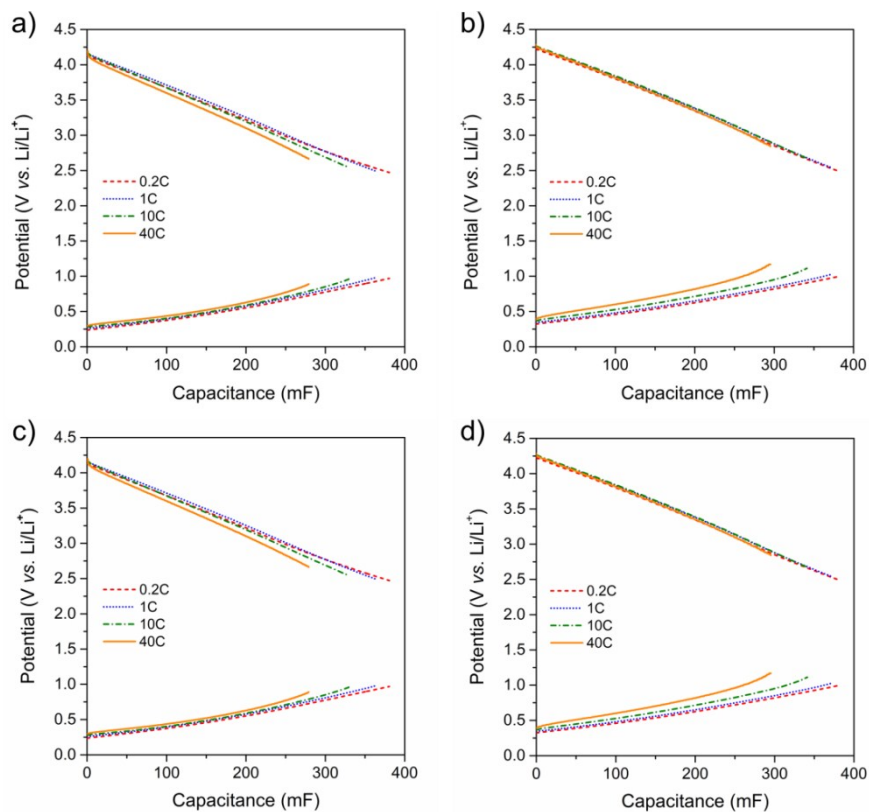


Fig. S11 Voltage behaviors of the PE and the NE in LIC full cells prepared by different Li^+ pre-doping methods at different current densities (0.2, 1.0, 10, and 40 C): (a) Li_6CoO_4 (60% doping), (b) metallic Li (60% doping), Li_6CoO_4 (100% doping), and (c) metallic Li (100% doping).

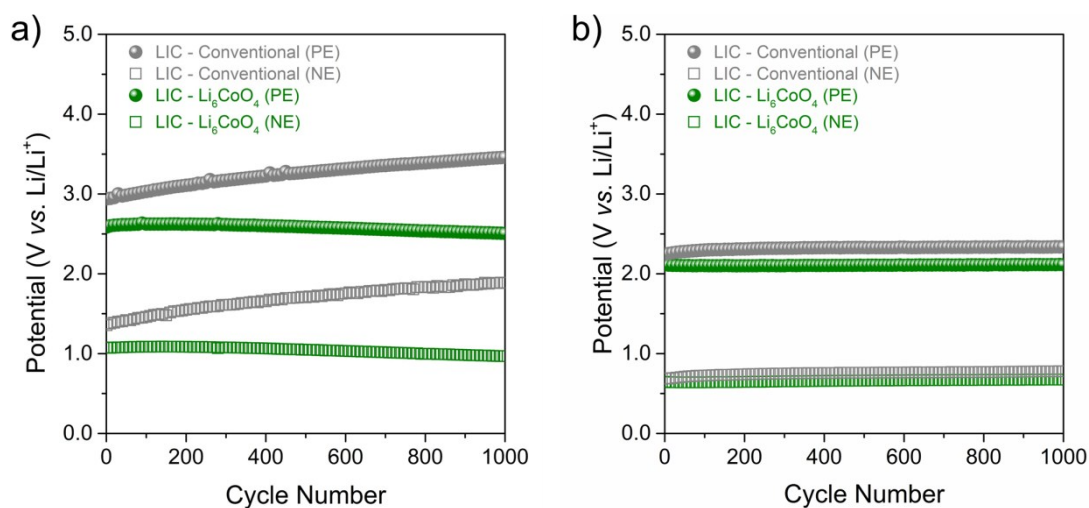


Fig. S12 Voltage behaviors of positive electrode and negative electrode in LIC full cells prepared by different Li^+ pre-doping methods during cycles: (a) 60% doping level and (b) 100% doping level.

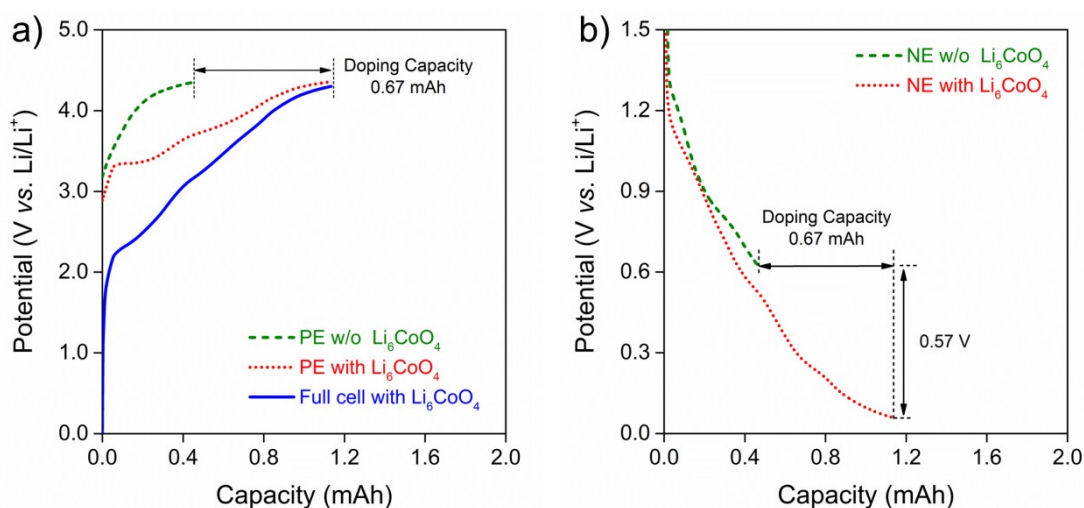


Fig. S13 Li⁺ pre-doping profiles (100% of practical NE capacity) of a LIC full cell with Li₆CoO₄ as an alternative Li⁺ source; corresponding voltage profiles of (a) the PE and (b) the NE during the first charge to 4.3 V vs. Li/Li⁺.

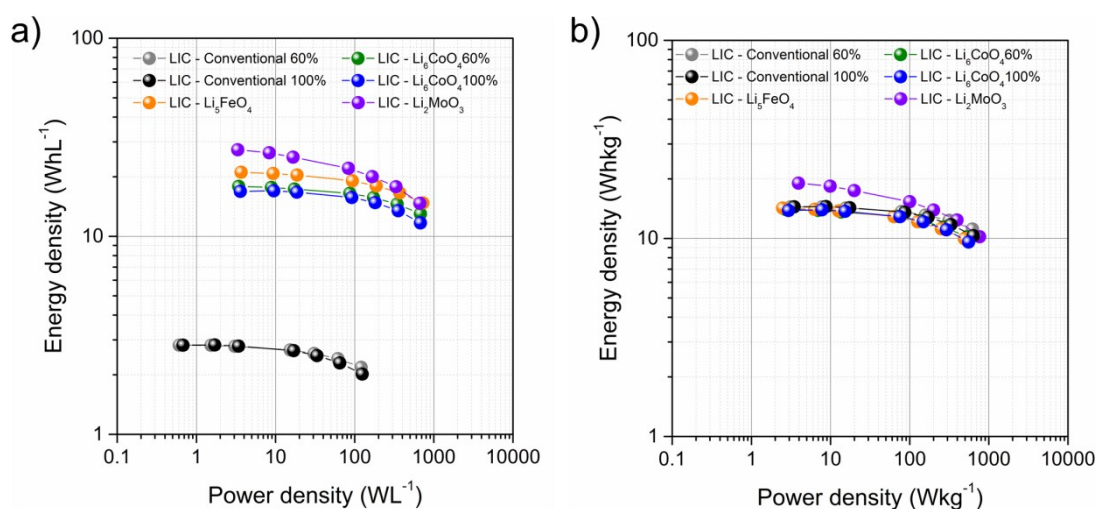


Fig. S14 Ragone plots of LIC full cells, containing Li₆CoO₄ and other candidates (Li₂MoO₃¹⁸ and Li₅FeO₄¹⁹) as alternative Li⁺ sources, compared with the conventional pre-lithiated with metallic Li (a) volumetric energy and power densities, and (b) gravimetric energy and power densities. The weight and volume of electrolyte and exterior materials of LIC full cell was excluded in the calculation.